J. Fluid Mech. (1990), *vol.* 215, *pp.* 125–143
Printed in Great Britain

On the stability of rivulet flow

By P. SCHMUKI† AND M. LASO‡
Absorption Technology, Sulzer Brothers Limited, CH-8401 Winterthur, Switzerland

(Received 4 April 1989 and in revised form 9 November 1989)

The aim of the present work is to investigate the existence regions of the different flow patterns exhibited by a liquid flowing down an inclined plane for a wide range of physical properties of the fluid (particularly surface tension and viscosity which were found to have the greatest influence). A model that predicts the decay frequency of oscillating or pendulum rivulets is presented. From this model, a stability criterion for the onset of oscillating rivulet flow is derived. Although the model does not contain any freely adjustable parameters, it shows good agreement with experimental measurements of rivulet decay frequency and of the transition point to pendulum rivulet. The transitions between different flow regimes are expected to cause drastic changes in heat and mass transfer rates between the liquid and the solid surface or between the liquid and the surrounding gaseous phase.

1. Introduction

The flow of a liquid down an inclined surface is of importance for a number of industrial processes, including gas–liquid contacting equipment in distillation and absorption, dry patch formation on heated surfaces, liquid film drainage from steam turbine stator blades, etc. For such a simple geometry, a relatively large number of hydrodynamic regimes can be easily observed, depending on the characteristics of the liquid and the solid surface.

An understanding of the individual flow regimes and of the transition points between them allows better prediction of heat and mass transfer rates in a variety of industrial processes and a rational design of packings for gas–liquid contacting devices.

The best known regime is probably the flow of a liquid on an inclined plane as a film. Over the last decades a large amount of work has been devoted to it, starting with the analysis by Nusselt (1916). However, the publications dealing with other flow regimes are surprisingly scarce. Some investigators (Hartley & Murgatroyd 1964; Bankoff 1970; Mikielewicz & Moszynski 1976) developed theories for film stability and breakdown which were the basis of much of the subsequent work on rivulet flow. Other publications, for example, Hobler & Czajka (1964) and Munakata, Watanabe & Miyashita (1975) have dealt with the problem of determining the minimum flow rate for complete surface wetting. Finally, a small number of workers have investigated the hydrodynamics of droplet and rivulet flow (Towell & Rothfeld 1966; Kern 1969; Nakagawa & Scott 1984; Doniec 1984; Dussan V. 1985). Most theoretical analyses are based on energetic considerations (Bankoff 1970; Mikielewicz

† Present address: Institut für Werkstoffchemie und Korrosion, Swiss Federal Institute of Technology, CH-8093 Zürich, Switzerland.

‡ Author to whom correspondence should be addressed. Present address: Institut für Polymere, Swiss Federal Institute of Technology, CH-8092 Zürich, Switzerland.

& Moszynski 1976; Hobler & Czajka 1964; Doniec 1988). Such analyses are based on the assumption that the stable flow regime will be found at a minimum of the total energy function, the definition of this energy function depending on the particular problem investigated. Other authors (Hartley & Murgatroyd 1964; Munakata *et al.* 1975) make use of dynamic considerations (equilibrium of forces) at the point of stagnation over the dry spot.

With respect to practical applications, most effort has been given to observing the conditions under which a thin liquid film driven along by gravity or shear stress applied at the free surface breaks into a series of rivulets. Hartley & Murgatroyd (1964), Bankoff (1970), Mikielewicz & Moszynski (1976) and Doniec (1988) used an energy criterion to describe film breakdown theoretically.

Some work has also been done on the subject of the meander region. Earlier authors like Tanner (1960) and Gorycki (1973) held helicoidal flow responsible for causing the meander-shaped stream. This thesis has been contradicted by Nakagawa (1982) and Nakagawa & Scott (1984). The same authors observed and qualitatively described the regions of existence of droplets and linear, meandering and oscillating rivulets depending on flow rate and surface slope but their work only describes one solid–liquid system (water/Plexiglas).

2. Qualitative description of the flow of a liquid down an inclined plane

The following qualitative discussion is meant solely to illustrate the different flow patterns and no specific values of the transition points between the different regimes will be given. A quantitative description will be presented in the next sections.

When a liquid flows down an inclined flat surface several different flow regimes can be observed, depending on the flow rate, the physical properties of the liquid–solid surface system and on the inclination of the surface.

Film flow is usually encountered in the flow of a 'well wetting' liquid down an inclined plane. This type of flow is characterized by a complete wetting of the surface by the liquid and by the absence of any dry spots (figure 1). This continuous film can be laminar or turbulent or it can present waves (see for example the work of Nusselt 1916; Benjamin 1957; Yih 1963). The flow regime is usually determined by means of the (conveniently simplified) Navier–Stokes equations. For stability analysis the Orr–Sommerfeld equation has been widely used.

If a 'non-wetting' liquid is considered, several different regimes can be observed as the flow rate of the liquid is increased. At very low flow rates, a series of droplets slide successively down the surface at a constant speed (figure 2). Dussan V. (1985) showed that the contact line between the droplet and the solid must contain straight portions. Her elegant theory is unfortunately limited to small contact angle hysteresis and does not take into account the viscosity of the liquid.

As the flow increases, the distance between two sliding droplets decreases until a point is reached where two successive droplets touch and a single straight laminar rivulet is formed (figure 3). This linear laminar rivulet (which can be considered as a special case of the film flow, see also Doniec 1988) has been the flow pattern best investigated after that of two-dimensional film flow. Kern (1969) and Towell & Rothfeld (1966) both described the shape and the velocity field of the linear laminar rivulet by simultaneously solving the Navier–Stokes and the meniscus equations. From this solution they derived the functional dependence of a characteristic rivulet dimension on the flow rate (Kern used the rivulet height, Towell & Rothfeld the width). Towell & Rothfeld give a relatively complicated general solution to the

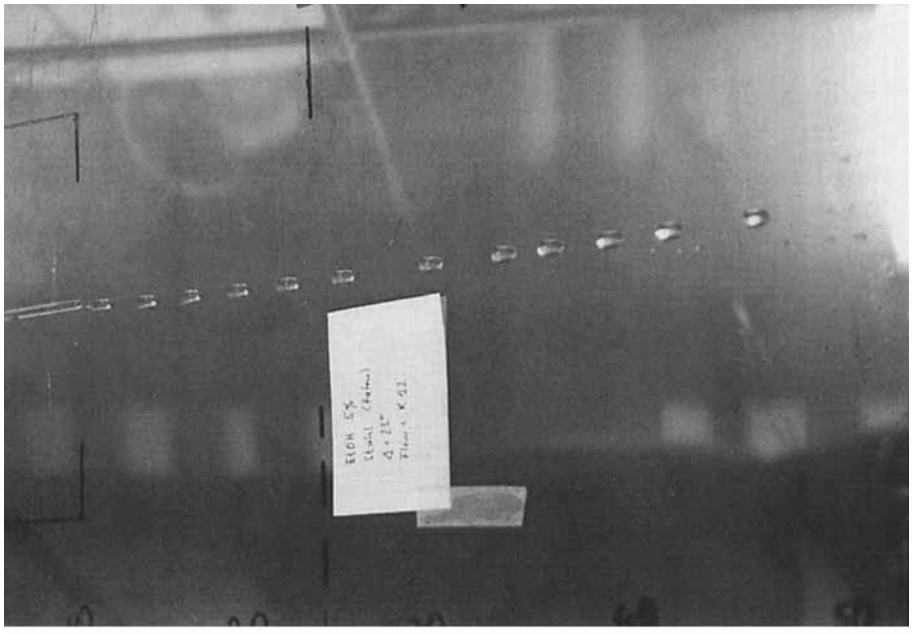

FIGURE 2. Droplet flow.

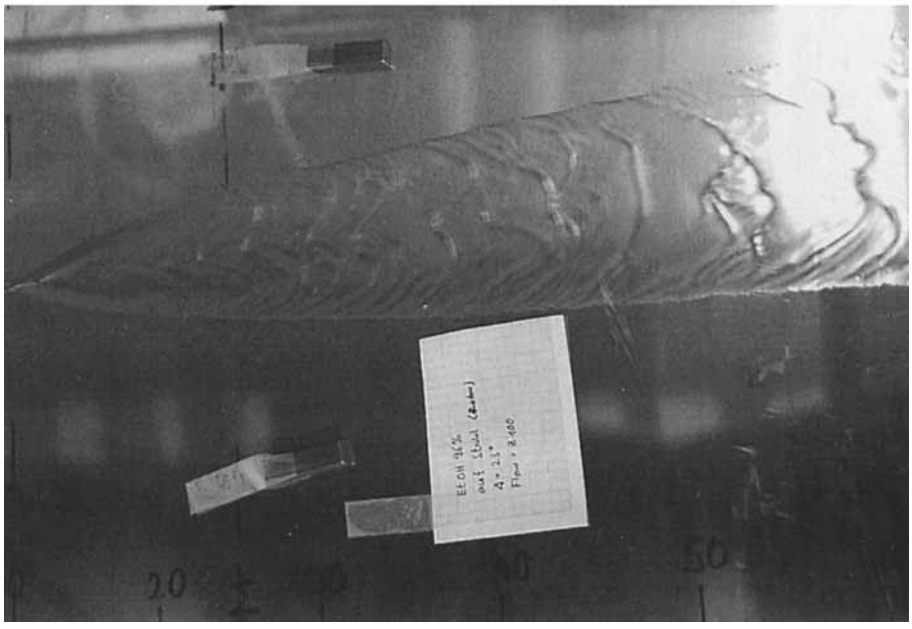

FIGURE 1. Flow of a wetting liquid down an inclined plane.

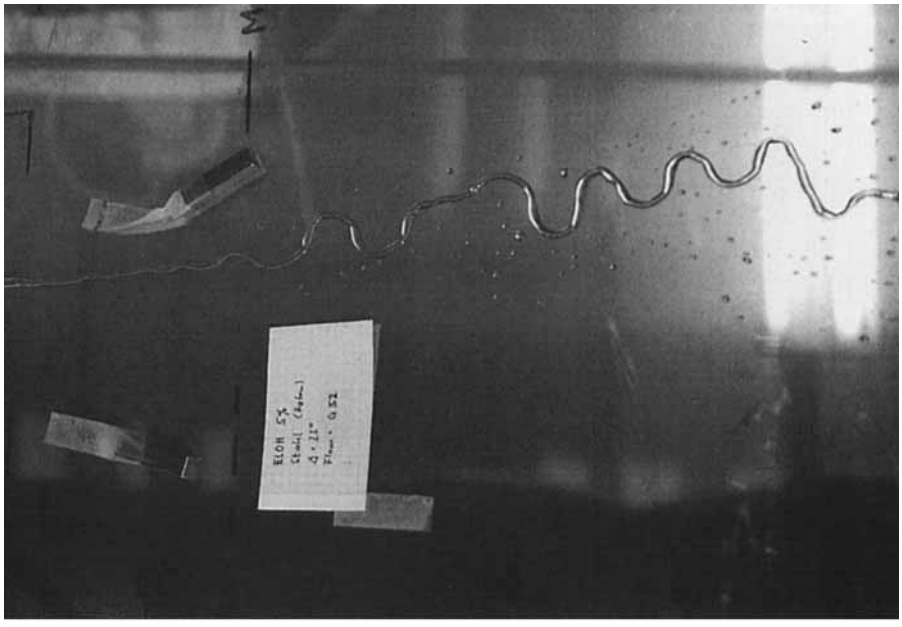

FIGURE 4. Meandering rivulet.

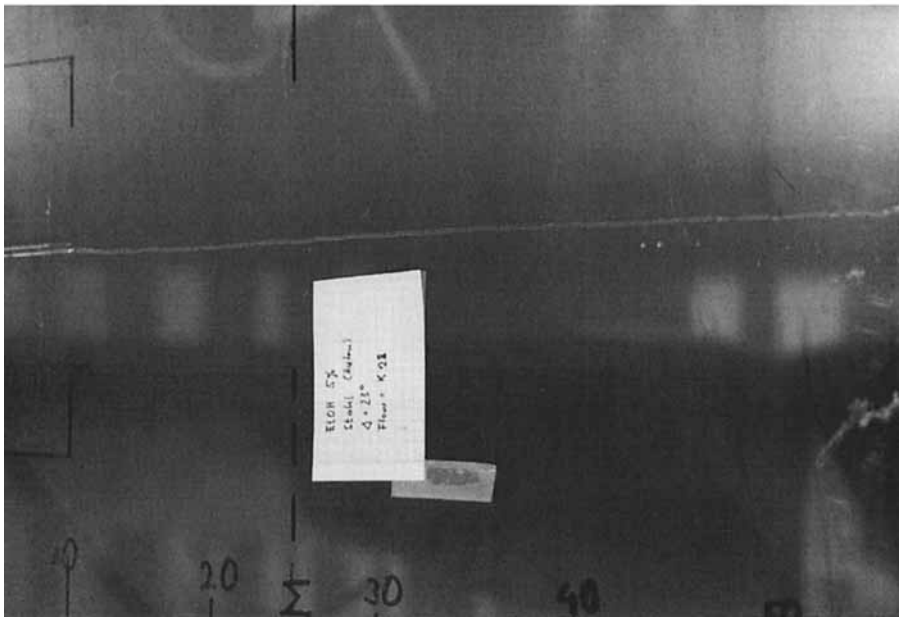

FIGURE 3. Linear rivulet.

FIGURE 5. Oscillating or pendulum rivulet.

problem but show that for systems with a 'bad wettability' the rivulet cross-section can be assumed to be a segment of a circle. For systems with a good wettability they showed that the general solution can be simplified by assuming a 'flat wide rivulet' of rectangular cross-section. The theory of Kern (1969) does not consider all the wettability parameters and is therefore suspected of being valid only for liquid–solid systems that have a similar wettability to the systems he investigated. The theory of Towell & Rothfeld not only considers the contact angle, it also describes the dependence of the rivulet flow on the inclination of the solid surface.

A further increase of the flow rate leads to an increase of the width and the height of the rivulet until another critical flow rate is reached where the straight laminar rivulet changes to a meandering stream composed of arcs of circles and some approximately straight sections (figure 4). The transition from linear to meandering rivulet is characterized by the appearance of waves of very small amplitude and wavelength. The characteristics of the rivulet (sinuosity, wavelength and amplitude of the waves) depend on the flow rate; for example, the wavelength and the amplitude grow as the flow rate increases. Nakagawa & Scott (1984) showed that contact-angle hysteresis is the most probable reason for meandering and helicoidal flow is only a consequence. Furthermore they showed qualitatively how the sinuosity

of the stream (the ratio of the total stream length to the length of the projection of the stream on the line of maximum slope of the surface) depends on the discharge rate and the surface slope.

If the flow rate exceeds another critical value, the meandering rivulet is no longer stable and a pendulum or oscillating rivulet (figure 5) is formed: the original rivulet decays and sheds several smaller ones at a constant rate. This rivulet decay frequency (number of sub-rivulets that are created per unit time) increases with increasing flow rate. Rivulet break-up is a dynamic process and therefore difficult to illustrate by means of a photograph. In spite of that, it is possible to see two subrivulets to the left of the main rivulet as well as a third one to the right that has just split off from the main rivulet. All these patterns can be observed once the liquid has flowed a certain distance downstream from the point at which it was brought onto the plate. This distance greatly depends on the liquid flow rate and on the way the liquid is brought onto the plate and can vary between a few millimetres for droplet flow to more than a metre for a linear turbulent rivulet.

A given solid–liquid system will display one or more of these regimes depending on the following variables: liquid density, viscosity, surface tension, contact angle between liquid and solid, plane inclination and liquid flow rate. For example, in the case of a liquid–solid system with a good wettability, only film flow exists over almost the whole plane inclination and flow rate ranges. For the flow of water over Plexiglas, droplet, rivulet, meandering rivulet and oscillating rivulet flows have been observed.

3. Experimental work

Figure 6 shows a schematic diagram of the experimental arrangement. The smooth test plates (AISI 316L stainless steel and polypropylene) were 1 m long and 0.5 m wide. The surface roughness was measured by the needle-scanning technique. Typical roughness values were in the range of 3 to 8×10^{-6} m. Several liquid systems were used in order to span as wide a range of physical properties as possible. Triethylene glycol, glycerol–water and ethanol–water mixtures of different compositions were employed to investigate the effects of viscosity and surface tension. The test liquid was released onto the centreline of the plate at a point 0.2 m down the slope from the upper edge through a smooth-ended glass tube of 0.005 m inner diameter and 0.15 m length. The liquid flowing down the plate was collected in a gutter and pumped into an overflow tank which permitted a constant discharge rate. The flow was controlled by a manual valve and a rotameter.

Since the contact angle and therefore the flow pattern were expected to be sensitive to the condition of the plate surface, special attention was given to the cleaning procedure. Before each run the plate was carefully prepared by wiping it with soft lint-free hygroscopic tissues and rinsing it with distilled water, ethanol and acetone. In this way, dust particles and any traces of the previous test system were removed. Additionally, an initially dry surface was found to be essential for reproducible measurements, otherwise the rivulet tended to follow paths that had already been wetted. For that reason the surface was dried 30 min prior to each run. It is important to note that a stainless steel surface that is clean is hydrophilic, completely wetted by water and should not have displayed any of the effects described in this paper. But a steel surface has a very high surface energy and it strongly attracts the oils which abound in its manufacturing environment. The cleaning process described here could not possibly have removed this very thin layer.

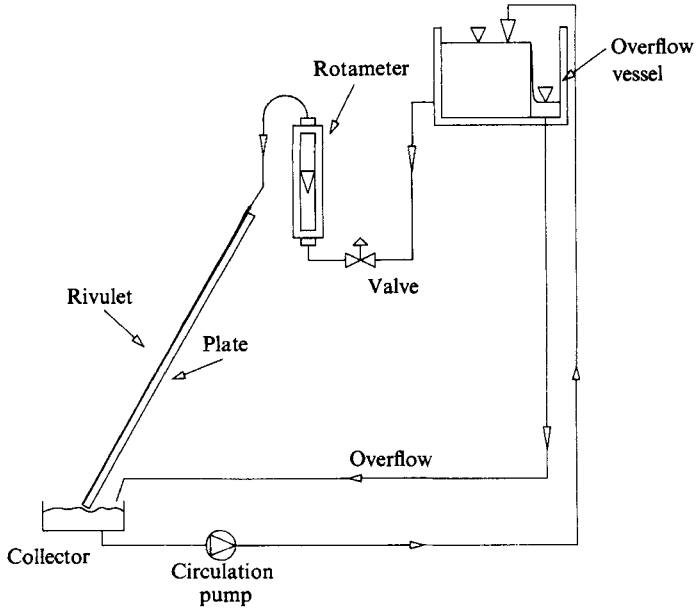

FIGURE 6. Schematic diagram of experimental arrangement.

Therefore, it must be assumed that an organic surface film covered the surface, making it hydrophobic. This does not invalidate the experiments, since the cleaning procedure did produce a reproducible surface which is the critical issue. Although this point does not materially affect the results, it is important to avoid any misconceptions concerning solid wettability.

The experimental variables which were independently varied were the liquid viscosity, surface tension and flow rate, the plate material and the inclination of the plate. For the different flow regimes, flow characteristics such as width and height of the rivulet and in the case of a pendulum rivulet, the rivulet decay frequency were measured.

The inclination of the plate was measured by a protractor to within 1°. The height of straight rivulets at their centreline was measured 0.20 m down stream from the glass tube mouth by means of a micrometer gauge. The micrometer was attached solidly to the plate and was carefully lowered from above the rivulet until its tip just touched the surface of the rivulet. This technique was precise enough to measure rivulet height to within 3×10^{-5} m. All experiments were recorded by a video-camera incorporating a macro-objective; the camera was placed perpendicular to the plate. The width of the rivulet was measured by comparing the size of its magnified image on the TV-screen to that of a reference scale placed on the plate surface beside the rivulet. Calibration runs showed that in this way the width of the rivulet could be measured to better than 5×10^{-5} m including focusing and parallax errors. The decay frequency (number of subrivulets that split off from the original one per unit time) was measured by counting the number of subrivulets in a given time (between 10 and 60 s, depending on the frequency). At high decay frequencies the video film was run in the slow motion mode and the timescale correspondingly corrected.

Contact angles were determined both statically and dynamically (see table 1). Static advancing and receding contact angle measurements were performed by determining the tangent to the (greatly magnified) profile of a sitting drop on the

	Steel	Polypropylene
Ethanol (96%) + Water (4%)	A: 9 R: <3 D: 8±4	A 23 R: 16 D: 25±6
Ethanol (28%) + Water (72%)	A: 39 R: 26 D: 41±6	A: 63 R: 47 D: 60±5
Triethyleneglycol (TEG)	A: 37 R: 25 D: 38±10	A: 59 R: 43 D: 58±8
Water	A: 62 R: 49 D: 68±8	A: 88 R: 82 D: 86±3
Ethanol (14%) + Water (86%)	A: 60 R: 48 D: 62±5	A: 71 R: 63 D: 69±5
Glycerin (60%) + Water (40%)	A: 68 R: 59 D: 67±8	A: 75 R: 64 D: 78±8

TABLE 1. Contact angles (in degrees) for some of the systems used (at 22 °C). A: advancing, R: receding, D: dynamic

horizontal plate. Dynamic measurements were made from the width and the heighth of a linear laminar rivulet by assuming the rivulet cross-section to be a segment of a circle. This assumption has been shown by Towell & Rothfeld (1966) to yield reasonably accurate results. For some of the systems important differences between static and dynamic measurements were found (see table 1). The accuracy of static contact angle measurements was estimated to be approximately 3° (two standard deviations). The accuracy of the dynamic measurements is included in table 1. It is interesting to note that the dynamic contact angles are very close to the static advancing contact angle in all cases; they can actually be considered to be identical within the experimental error. Furthermore, Nakagawa & Scott (1984) showed that dynamic contact angles can vary along the rivulet, most probably due to microscopic surface imperfections. Since the dynamically measured values were thought to be more representative of the actual flow conditions they were used throughout this work. Fortunately, the equations describing rivulet behaviour are not strongly sensitive to the value of the contact angle above 15° and therefore an experimental uncertainty of a few degrees does not introduce large errors.

4. Results

4.1. *Stability domains and transition points*

For the system stainless steel/water all the flow patterns depicted in figures 1–5 could be observed for all plate inclinations, including vertical plates, and independently of the way the liquid was brought onto the plate. These flow patterns were found to be stable within certain ranges of physical properties, plate inclination and plate material. Relatively sharp transitions exist between the different stability domains.

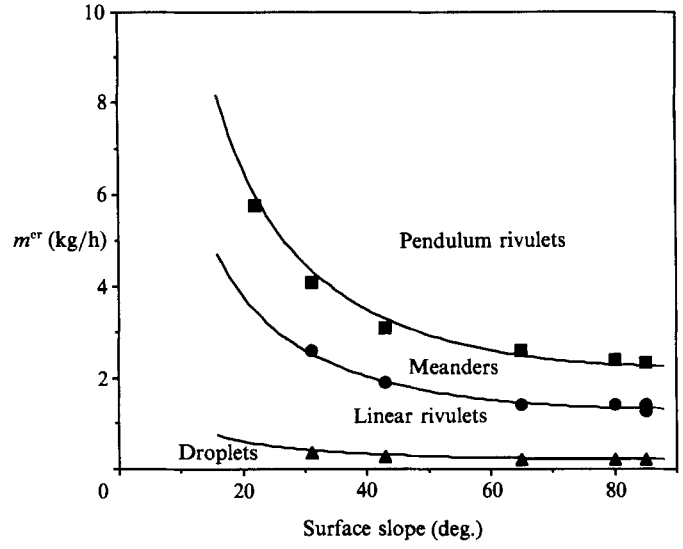

FIGURE 7. Stability domains as a function of plate inclination. ■, transition from meander to pendulum rivulet; ●, transition from linear rivulet to meander; ▲, transition from droplets to linear rivulet.

Given the large number of independent variables, it is difficult to give a concise representation of the multidimensional stability regions.

4.1.1. *Influence of plate inclination*

Figure 7 shows the influence of plate inclination and flow rate on the existence domains, the abscissa and the ordinate being surface slope and liquid discharge rate respectively. It is apparent from this figure that as the surface slope increases, all the transitions occur at lower flow rates.

The simplest explanation for this effect is that the transition points of a given system depend only on the component of gravity parallel to the plate surface. Under this assumption one would expect the relationship

$$m_{\mathrm{v}} = m_{\alpha} \sin \alpha, \tag{1}$$

to hold, where m_{v} and m_{α} represent the transition flow rates for a vertical plate and for a plate inclination of angle α respectively. (Such a dependence has been shown by Allen & Biggin (1974) to hold for the discharge rate of a straight laminar rivulet.) The curves in figure 7 were drawn by converting the transition flow rates at 90° to other inclinations by means of (1).

The possibility of scaling the transition points to 90° (or to any other reference value) is very convenient, because one of the free parameters can be eliminated: it is only necessary to measure the transition points for a given plate inclination; the corresponding values at different inclinations can then be determined by means of (1), other things being equal. For this reason it was decided to work with a single inclination angle (70°) for the rest of the experiments.

4.1.2. *Influence of viscosity and surface tension*

Figures 8 and 9 illustrate the influence of viscosity and surface tension respectively on the transition points for the stainless steel surface. Viscosity and surface tension ranges were investigated by varying the concentration of glycerol–water and

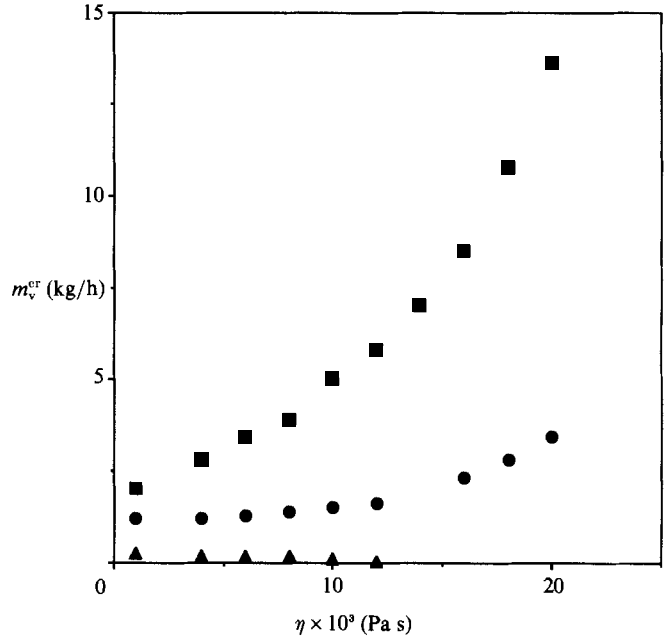

FIGURE 8. Effect of viscosity on stability domains. For key see figure 7.

ethanol–water mixtures. Adding glycerol to water increases the viscosity drastically without altering the surface tension significantly. The addition of ethanol greatly reduces the surface tension without affecting the viscosity too much. Figures 8 and 9 can only be considered as semiquantitative because strictly speaking, two parameters are being changed simultaneously.

Figure 8 represents the transition flow rates (measured at an inclination angle of 70° and referred to the vertical plate) as a function of viscosity for an almost constant σ of about 0.070 N/m. The transition points were found to increase with increasing viscosity except for the transition from droplet flow to linear rivulet. The droplet flow region vanished as the viscosity of the liquid increased: since the droplet size is mainly controlled by surface tension and its speed down the plate by viscosity, there must be a combination of μ and σ at which the diameter of the drop is equal to the distance between the centres of two consecutive drops, so that all drops merge into a single rivulet. For glycerol–water mixtures (σ between 0.06 and 0.07 N/m) this happened at about 0.012 Pa s. For liquids of μ greater than about 0.020 Pa s the transition points were difficult to observe (owing among other things to very small wave amplitudes of the meandering rivulet and to very long transients until the liquid settled into a stable flow pattern). Experiments with liquids of even higher viscosities indicate that for very viscous liquids only the linear rivulet domain exists (this would correspond to a vertical asymptote in figure 8). The exact value at which the other domains vanish depends of course on the density and surface tension of the liquid and the nature of the surface.

Figure 9 represents the transition flow rates (measured at an inclination angle of 70° and referred to the vertical plate) as a function of surface tension (for an almost constant μ of about 0.001 Pa s). The transition points between the different flow patterns pass through a relatively flat minimum at about 0.045 N/m. It is interesting to note that there is again a value of the surface tension (in this case about

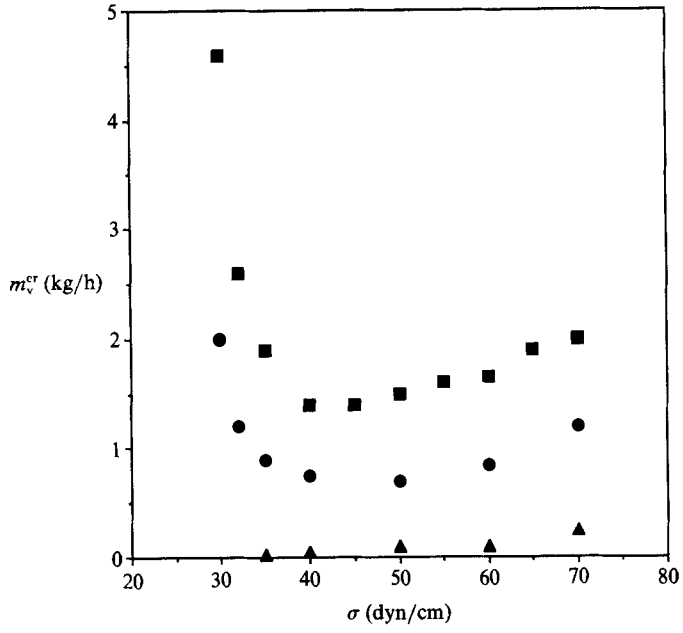

FIGURE 9. Effect of surface tension on stability domains. For key see figure 7.

0.029 N/m) below which no droplet, meandering or oscillating rivulet flow exist and the linear rivulet domain grows. At even lower surface tensions, the linear broad rivulet is indistinguishable from film flow (owing to the good wettability).

4.2. *Decay frequency of oscillating rivulets*

If the flow rate of a meandering rivulet was increased beyond the transition point, a new flow pattern appeared: the oscillating or pendulum rivulet. This flow was characterized by a periodic decay of the unstable main meandering rivulet in several smaller ones which flowed as virtually straight rivulets. These subrivulets were found to be all of the same size within the measurement error (analysis of video films). The transition is thought to be accompanied by a dramatic increase in heat and mass transfer between the plate and the liquid and/or between the liquid and the surrounding gaseous phase. Thus, the prediction of the transition point and of the decay frequency is of importance for the understanding of heat and mass transfer processes.

Figure 10 shows some experimental values of the rivulet decay frequencies (measured at $\alpha = 70°$) for a variety of liquid/solid systems as a function of the mass flow rate, referred to the vertical plate. As wide a range as possible of flow rates, physical properties (viscosity and surface tension) and different surfaces were investigated. It can be seen that all these parameters have a large effect on the decay frequency. As expected, and for the same flow rate and physical properties, bad wettability leads to higher oscillation frequencies. The influence of liquid flow rate on decay frequency is fairly clear: the decay frequency increases approximately linearly with increasing flow rate. However, no straightforward dependence on viscosity and surface tension can be deduced from figure 10.

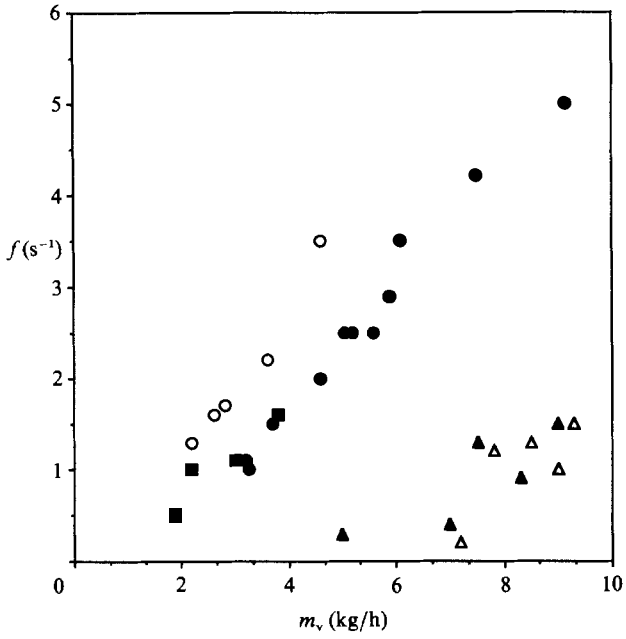

FIGURE 10. Decay frequencies of oscillating rivulets as a function of liquid discharge rate. ●, water on steel; ○, water on polypropylene; ▲, glycerol 60 % on steel; △, glycerol 60 % on polypropylene; ■, ethanol 27 % on polypropylene.

5. Theoretical approach

In the following, a model is presented that attempts to predict the transition point from a single rivulet to an oscillating (pendulum) rivulet configuration and furthermore how the rivulet decay frequency depends on the discharge rate and the physical properties of the system.

The present model is based on an energy criterion: the transition is postulated to occur when the rivulet flow ceases to be stable, that is, when the total energy of the single rivulet can be lowered by its decaying in several smaller ones (subrivulets). Therefore the strategy is to formulate the total energy of the system and then to find the minimum value of this energy as a function of the number of subrivulets for a given total flow rate.

5.1. *Stability of a rivulet*

In order to compute the energy of the system, an adequate representation of the rivulet has to be used. Doniec (1984) studied film breakdown by describing the exact rivulet profile shape; Mikielewicz & Moszynski (1976) and Bankoff (1971) assumed the rivulet cross-section to be a segment of a circle. A comparison of their results shows the latter approximation to be an adequate one, in agreement with Towell & Rothfeld's (1966) analysis. Allen & Biggin (1974) obtained the exact velocity field by solving the full Poisson equation by the finite elements method and concluded that the rivulet has an inner 'core' where the flow is basically that of a two-dimensional thin film. They showed that the zero-order solution of Towell & Rothfeld (1966) gives a good representation of the flow profile except in the neighbourhood of the gas–liquid interface. Therefore in this work the cross-section of a rivulet was considered to be a segment of a circle of radius R as shown in figure 11. The height of the rivulet $h(x)$, where h is the rivulet thickness at a horizontal distance x from the

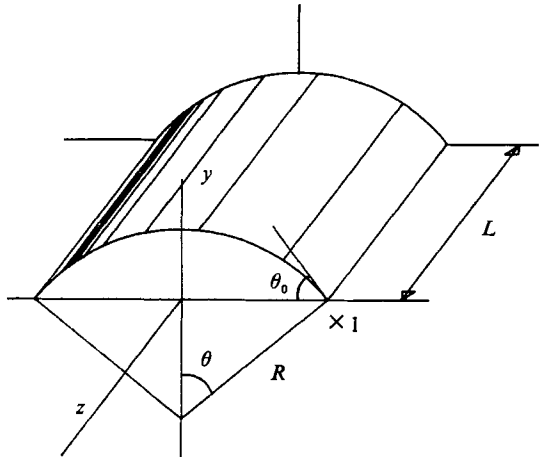

FIGURE 11. Simplified rivulet model.

centre is given, in terms of the polar subtended angle θ, by

$$h(x) = R(\cos\theta - \cos\theta_0), \tag{2}$$

where θ_0 is the solid–liquid contact angle. The velocity profile in the rivulet is (Bankoff 1971):

$$u(x,y) = \beta(\tfrac{1}{2}y^2 - yh(x)) \quad \left(\beta = \frac{g\rho}{\mu}\right). \tag{3}$$

The implicit assumption in (3) is that the velocity profile in each slice of width $\mathrm{d}x$ and thickness $h(x)$ is that of a uniform film of the same thickness (the inaccuracy incurred by using such an approximation was found to be smaller than the experimental error in the determination of the transition points). The volumetric discharge rate of the rivulet is then

$$Q = 2\int_0^{x_1}\int_0^{h(x)} u(x,y)\,\mathrm{d}y\,\mathrm{d}x = \tfrac{2}{3}\beta R^4 f(\theta_0), \tag{4}$$

where

$$f(\theta) = \int_0^{\theta_0} (\cos\theta - \cos\theta_0)^3 \cos\theta\,\mathrm{d}\theta$$

$$= -\tfrac{1}{4}\cos^3\theta_0 \sin\theta_0 - \tfrac{13}{8}\cos\theta_0\sin\theta_0 - \tfrac{3}{2}\theta_0\sin^2\theta_0 + \tfrac{15}{8}\theta_0. \tag{5}$$

The total energy of the system composed of a rivulet segment of length L and the associated dry surface is given by the sum of the kinetic and potential energy of the rivulet and the surface energy of the liquid–gas and solid–gas interfaces. The potential energy can be shown to be negligible on all accounts for the systems used and was not considered in the present study: even for a liquid of high density and surface tension like mercury, it amounts to less than 1% of the kinetic energy at inclinations $\alpha > 5°$.

Therefore:

$$E = \tfrac{1}{2}\rho L A\bar{u}^2 + 2RL\theta_0\sigma_{1g} + 2RL\sin\theta_0(\sigma_{sl} - \sigma_{sg}), \tag{6}$$

where:

$$A = \tfrac{1}{2}R^2(2\theta_0 - \sin 2\theta_0), \tag{7}$$

and from (4) the mean velocity is:

$$\bar{u} = \frac{Q}{A} = \frac{4}{3}\frac{f(\theta)}{(2\theta_0 - \sin 2\theta_0)}\beta R^2. \tag{8}$$

Subscript lg indicates liquid–gas interface, sl, solid–liquid interface and sg, solid–gas interface. Employing the Young and Dupres equation:

$$(\sigma_{sl}-\sigma_{sg}) = -\sigma_{lg}\cos\theta_0, \tag{9}$$

the second term in the surface energy equation can be simplified. The use of the Young and Dupres equation implies the uniqueness of the contact angle, which is then a parameter that relates the various thermodynamically defined surface tensions. However, in our experiments, this angle could not be measured unambiguously, as shown by the differences between the advancing and receding contact angles (hysteresis). This is in disagreement with Young's equation which admits of but one value of the contact angle for any given system at equilibrium. In spite of this inconsistency, we used the Young and Dupres equation because of its simplicity and because the effect of the hysteresis is not very significant if the contact angle is greater than about 15° (that is, there is not a large difference in the total energy of the rivulet computed using the advancing and the receding contact angles). Substituting equations (7), (8) and (9) in (6), the total energy in terms of R is obtained.

$$E = \frac{2}{9}\frac{[f(\theta)]^2}{(\theta_0-\sin\theta_0\cos\theta_0)}\beta^2\rho L R^6 + 2RL\sigma_{lg}(\theta_0-\sin\theta_0\cos\theta_0). \tag{10}$$

Solving relationship (4) for R and replacing in (10)

$$E = (\tfrac{3}{2})^{1.5}\tfrac{2}{9}\rho L\beta^{0.5}\frac{[f(\theta)]^{0.5}}{(\theta_0-\sin\theta_0\cos\theta_0)}Q^{1.5} + 2(\tfrac{3}{2})^{0.25}\frac{L\sigma_{lg}}{\beta^{0.25}}\frac{(\theta_0-\sin\theta_0\cos\theta_0)}{f(\theta)^{0.25}}Q^{0.25}. \tag{11}$$

The total energy of n rivulets having the same total volumetric flow rate as the original is therefore:

$$E_{tot} = nE_n \quad \text{with} \quad Q_n = \frac{Q_{tot}}{n}. \tag{12}$$

For the single rivulet to be stable, the total energy of the system formed by n rivulets (which is a function of n) must not exhibit a minimum at $n > 1$ (if such a minimum existed, the configuration formed by n rivulets would be more stable than the single rivulet). Or, expressed in a different way, it is impossible for one rivulet to divide into two or more rivulets if E_{tot} is an increasing function of n for $n > 1$. Thus, substituting E and Q from (12):

$$E_{tot} = n\left(B\left(\frac{Q}{n}\right)^{1.5} + C\left(\frac{Q}{n}\right)^{0.25}\right), \tag{13}$$

where B and C represent the prefactors (functions of the physical properties and contact angle) in (11). (A more general form of the equation representing the total energy could have been written if analytical expressions for the area and perimeter of the rivulet were available. Since the assumption of circular cross-section is a good approximation below Ω^{cr} as defined in (31) and leads to analytically tractable expressions, it was the approach we followed. The good agreement with the experimental results justifies this procedure. The rigorous approach remains of course open to a fully numerical solution, but no significant accuracy return on the computational investment can be expected.)

Differentiating the total energy with respect to n, equating to zero and solving for n gives:

$$n = \left(\frac{2B}{3C}\right)^{0.8}Q. \tag{14}$$

The transition point to oscillating rivulet flow (decay of the main rivulet into several subrivulets) will be attained when $n = 1$, leading to the critical flow rate Q^{cr}:

$$Q^{cr} = \left(\frac{3C}{2B}\right)^{0.8} = 5.348 \frac{\sigma_{lg}^{0.8}\mu^{0.6}}{\rho^{1.4}g^{0.6}} \frac{(\theta_0 - \sin\theta_0\cos\theta_0)^{1.6}}{f(\theta_0)}. \tag{15}$$

In order to transform above equation in a dimensionless form we introduce the Reynolds number:

$$Re = \frac{\bar{u}4h\rho}{\mu}, \tag{16}$$

where h is the maximum height of the rivulet.

$$h = R(1 - \cos\theta_0). \tag{17}$$

Solving (4) for R, substituting into (17) and (8) and replacing these terms in (16), we obtain the dependence of the Reynolds number on the volumetric flow rate:

$$Re = 4(\tfrac{2}{3})^{0.25} \frac{(1-\cos\theta_0)}{(\theta_0 - \sin\theta_0\cos\theta_0)} [f(\theta)]^{0.25} \frac{\beta^{0.25}\rho}{\mu} Q^{0.75}. \tag{18}$$

Setting $Q = Q^{cr}$ (equation (14)) the critical Reynolds number is:

$$Re^{cr} = 12.71 \frac{\rho^{0.2}\sigma_{lg}^{0.6}}{g^{0.2}\mu^{0.8}} \frac{(1-\cos\theta_0)(\theta_0 - \sin\theta_0\cos\theta_0)^{0.2}}{f(\theta)^{0.2}}. \tag{19}$$

We now introduce the dimensionless capillary-buoyancy number K_F:

$$K_F = \frac{g\mu^4}{\rho\sigma_{lg}^3}, \tag{20}$$

and hence (19) becomes:

$$Re^{cr} = 12.71 K_F^{-0.2} F(\theta), \tag{21}$$

were $F(\theta)$ represents the contact angle factor in (18); or if we introduce the modified critical Reynolds number, Re_{mod}^{cr}

$$Re_{mod}^{cr} = \frac{Re^{cr}}{F(\theta)} = 12.71 K_F^{-0.2}. \tag{22}$$

5.2. *Rivulet decay frequency*

The rivulet decay frequency f is defined as the number of subrivulets in which the main rivulet decays per unit time, that is, the number of subrivulets shed by the main rivulet per unit time:

$$f = \frac{n-1}{\Delta t}. \tag{23}$$

To represent this frequency, we introduce the dimensionless Strouhal number N_{St}:

$$N_{St} = f\Delta t = n - 1, \tag{24}$$

and hence using (14):

$$N_{St} + 1 = \left(\frac{2B}{3C}\right)^{0.8} Q. \tag{25}$$

Solving (17) for Q and introducing into (23) leads to:

$$N_{St} + 1 = 0.03371 \left(\frac{g\mu^4}{\rho\sigma_{lg}^3}\right)^{0.266} \left(\frac{f(\theta)}{(1-\cos\theta_0)^5(\theta_0 - \sin\theta_0\cos\theta_0)}\right)^{0.266} Re^{1.333}. \tag{26}$$

Considering (20) and $F(\theta)$

$$N_{St}+1 = 0.033\,71 K_F^{0.266} F(\theta)^{1.333} Re^{1.333}, \tag{27}$$

and introducing the dimensionless frequency parameter ω, the following relationship between frequency and flow rate is found:

$$\omega = \frac{N_{St}+1}{K_F^{0.266} F(\theta)} = 0.033\,71\, Re^{1.333}. \tag{28}$$

6. Discussion

In this section the applicability of several published theories as well as of our own model is discussed, with respect to the experimental results.

6.1. *Plate inclination*

As has been shown in figure 7, the effect of plate inclination on the transition points between different flow regimes can be suitably described by means of (1). A similarly good agreement with the experimental values for all transition points was found in all runs, which substantiates the validity of (1).

The investigation of the transition lines for the system polypropylene–water led to the same relationship (1), having, of course, different transition flow rates for a given inclination owing to the different wettability characteristics.

Nakagawa & Scott (1984) qualitatively described their transition curves for Plexiglas/water as linear (transition from droplet flow to meandering rivulet) or exponential (transition from meandering to oscillating rivulet). However an evaluation of their published data shows them to be consistent with the sinous relationship (1) as well.

According to Towell & Rothfeld (1966), two limiting rivulet shapes can be distinguished, leading to two different functional dependencies between the dimensionless rivulet width P and the dimensionless flow rate Ω:

(*a*) for a small rivulet of approximately circular cross-section:

$$P^4 = 24\Omega \frac{\sin^4\theta_0}{f(\theta)}, \tag{29}$$

(*b*) for a wide flat rivulet:

$$P = \tfrac{3}{8}\Omega \frac{1}{\sin^3(\frac{1}{2}\theta_0)}, \tag{30}$$

where

$$P = b\left(\frac{\rho g \cos\alpha}{\sigma_{lg}}\right)^{0.5}, \quad \Omega = \frac{\mu\rho g Q}{\sigma_{lg}^2}\cot\alpha\cos\alpha.$$

One of these two limiting cases was found to hold for all values of Ω except in a relatively narrow transition region. The transition or critical flow rate Ω^{cr} can be obtained by finding the intersection of (29) and (30):

$$\Omega^{cr} = 26.89\left(\frac{\cos(\frac{1}{2}\theta_0)\sin^4(\frac{1}{2}\theta_0)}{f(\theta)^{0.25}}\right)^{1.33}. \tag{31}$$

Hence, for a given system, the shape of the rivulet at values of Ω below Ω^{cr} can be expected to be a sector of a circle. Figure 12 shows a plot of P versus Ω for two solid–liquid systems with very different wettability characteristics. Points lying above Ω^{cr} and fitting (30) can only be found in the case of a solid–liquid system with

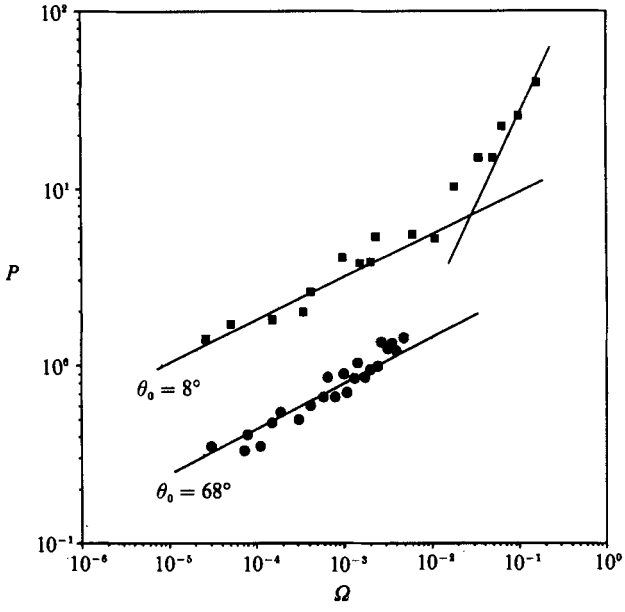

FIGURE 12. Rivulet width as a function of liquid discharge rate (dimensionless). Continuous lines represent predictions of Towell & Rothfeld's theory. ■, EtOH 96% on stainless steel; ●, water on stainless steel.

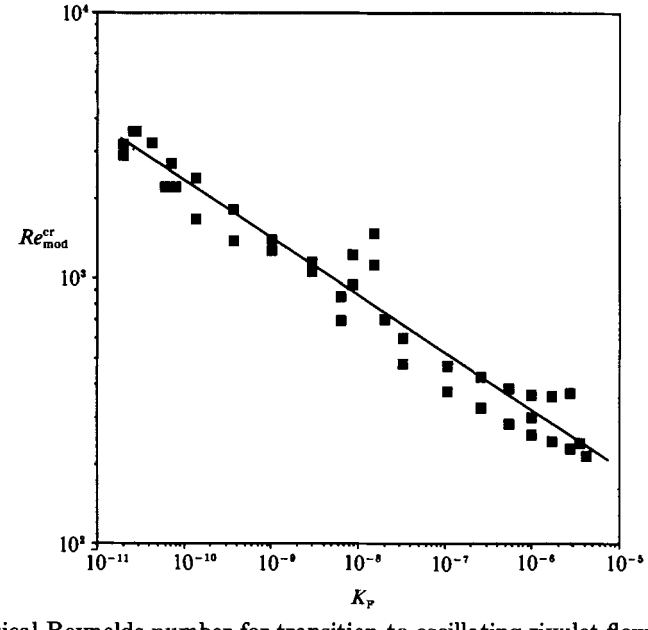

FIGURE 13. Critical Reynolds number for transition to oscillating rivulet flow as a function of the capillary-buoyancy number K_F. Continuous line represents theoretical predictions according to (22).

good wettability, like 96% ethanol on stainless steel. The stability and decay frequencies of rivulets represented by points above Ω^{cr} cannot be predicted by the theory presented, since the assumption of a circular rivulet cross-section no longer holds. In the case of a bad wetting system, e.g. water on stainless steel, the flat wide rivulet region cannot be reached since the rivulet flow becomes unstable below Ω^{cr}.

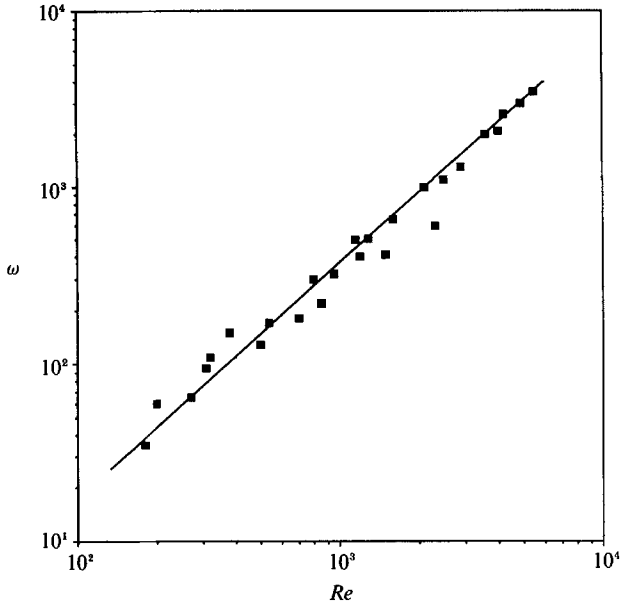

FIGURE 14. Oscillating rivulet decay frequency as a function of liquid discharge rate (dimensionless). Line represents theoretical predictions according to (28).

In order to estimate the applicability of the present theory to the transition from meandering to oscillating rivulet flow, the experimental points were plotted together with the theoretical prediction of (22). The points correspond to different liquid–solid systems (note that K_F depends on the physical properties and can only be modified by using liquid–solid systems with different physical properties). The accuracy of the experimental values is influenced by some of the transition points not being very sharply defined and by contact angle hysteresis as described for instance by Blake & Haynes (1973).

The agreement between experiment and theory is good, especially in view of the fact that (22) was derived from first principles and does not contain any adjustable parameters. Besides, (22) correctly accounts for the large differences in viscosity, surface tension and solid wettability between the different systems. The points deviating from the curve at $K_F = 10^{-8}$ correspond to systems whose transition point lies above Ω^{cr}, that is, where the rivulet cross-section is not any more a sector of a circle and the theory cannot apply.

It should be noted here that the theory is actually based on an analysis of the stability of a straight rivulet and does not consider the intermediate flow pattern of a meandering stream. This may explain the fact that the theory predicts transition points slightly higher than the experimental ones as shown in figure 13. Nakagawa & Scott (1984) showed that meanders have an asymmetrical cross-section and hence an asymmetrical velocity profile which may cause a split-off of subrivulets at lower flow rates than expected.

The results obtained from the theory for the decay frequency of oscillating rivulets are presented in figure 14. The experimental dimensionless decay frequencies (frequency parameter) are plotted against the Reynolds number. The predictions of (28) are shown as a solid line. Again, the theoretical predictions closely match the experimental values for a large number of liquid–solid systems and flow rates, even though (28) does not contain freely adjustable parameters.

7. Conclusions

A theoretical model for rivulet flow stability was presented which is able to predict rivulet instability (transition to meandering rivulet) and decay frequency as a function of physical properties and flow rate. The validity of this model is limited to solid–liquid systems below Ω^{cr}, that is, it does not apply to flat wide rivulets of almost rectangular cross-section. The model does not contain freely adjustable parameters and shows very satisfactory agreement with experimental data.

REFERENCES

ALLEN, R. F. & BIGGIN, C. M. 1974 Longitudinal flow of a lenticular liquid filament down an inclined plane. *Phys. Fluids* **17**(2), 287–291.

BANKOFF, S. G. 1971 Minimum thickness of a draining film. *J. Heat Mass Transfer* **14**, 2143–2146.

BENJAMIN, T. B. 1957 Wave formation in laminar flow down an inclined plane. *J. Fluid Mech.* **2**, 554–574.

BLAKE, T. D. & HAYNES, J. M. 1973 Contact angle hysteresis. *Prog. Surface Membrane Sci.* **6**, 125–138.

DONIEC, A. 1984 Laminar flow of a liquid down a vertical solid surface. Maximum thickness of liquid rivulet. *PhysicoChem. Hydrodyn.* **5**(2), 143–152.

DONIEC, A. 1988 Flow of a laminar film down a vertical surface. *Chem. Engng Sci.* **43**(4), 847–854.

DUSSAN V., E. B. 1985 On the ability of drops or bubbles to stick to non-horizontal surfaces of solids. Part 2. Small drops of bubbles having contact angles of arbitrary size. *J. Fluid Mech.* **151**, 1–20.

GORYCKI, M. A. 1973 Hydraulic drag: a meander-initiating mechanism. *Bull. Geol. Soc. Am.* **84**, 175–186.

HARTLEY, D. E. & MURGATROYD, W. 1964 Criteria for the break-up of thin liquid layers flowing isothermally over solid surfaces. *J. Heat Mass Transfer*, **7**, 1003–1015.

HOBLER, T. & CZAJKA, J. 1968 Minimum wetting rate of a flat surface. *Chemia Stosow.* **2B**, 169–186.

KERN, J. 1969 Zur Hydrodynamik der Rinnsale. *Verfahrenstechnik* **3**(10), 425–430.

MIKIELEWICZ, J. & MOSZYNSKI, J. R. 1976 Minimum thickness of a liquid film flowing vertically down a solid surface. *J. Heat Mass Transfer* **19**, 771–776.

MUNAKATA, T., WATANABE, K. & MIYASHITA, K. 1975 Minimum wetting rate on wetted-wall column. Correlation over wide range of liquid viscosity. *J. Chem. Engng Japan* **8**(6), 440–444.

NAKAGAWA, T. 1982 On role of discharge in sinuosity of stream on a smooth plate. *Naturwissenschaften* **69**, 142.

NAKAGAWA, T. & SCOTT, J. C. 1984 Stream meanders on a smooth hydrophobic surface. *J. Fluid Mech.* **149**, 89–99.

NUSSELT, W. 1916 Die Oberflächenkondensation des Wasserdampfes. *Z. Verein deutscher Ingenieure* **60**, 541.

TANNER, W. F. 1960 Helicoidal flow, a possible cause of meandering. *J. Geophys. Res.* **63**(3), 993.

TOWELL, G. D. & ROTHFELD, L. B. 1966 Hydrodynamics of rivulet flow. *AIChE J.* **12**(5), 972.

YIH, C.-S. 1963 Stability of liquid flow down an inclined plane. *Phys. Fluids* **6**(3), 321–334.